

Czech Technical University in Prague

Faculty of Mechanical Engineering

Institute of Aircraft Technology



MASTER'S THESIS

Validation of Temperatures in a Thermal-Vacuum Chamber

Validace teplot v termálně-vakuové komoře

Bc. Matěj Koubek

Thesis Supervisor: Ing. Jaromír Kučera

Study Programme: N3958 Aviation and Astronautics

Field of Study: 3906T008 Aircraft and Space Technology

Prague 2021

I. OSOBNÍ A STUDIJNÍ ÚDAJE

Příjmení: **Koubek** Jméno: **Matěj** Osobní číslo: **456364**
Fakulta/ústav: **Fakulta strojní**
Zadávací katedra/ústav: **Ústav letadlové techniky**
Studijní program: **Letectví a kosmonautika**
Studijní obor: **Letadlová a kosmická technika**

II. ÚDAJE K DIPLOMOVÉ PRÁCI

Název diplomové práce:

Validace teplot v termálně-vakuové komoře

Název diplomové práce anglicky:

Validation of temperatures in a thermal-vacuum chamber

Pokyny pro vypracování:

- 1) Proveďte rešerši stávajících návrhových a realizačních metod pro termálně-vakuové cyklování (TVC)
- 2) Zvolte metodu pro simulaci TVC vhodnou pro stávající temperační plášť
- 3) Proveďte simulaci TVC protokolu
- 4) Proveďte experimentální ověření simulací získaných teplot v zařízení

Seznam doporučené literatury:

Malcolm Macdonald, Viorel Badescu (ed.): The International Handbook of Space Technology, Springer, 2014, ISBN 978-3-642-41101-4
Vincent L. Pisacane: The space environment and its effects on space systems, AIAA, 2008, ISBN 978-1-56347-926-7
European Cooperation for Space Standardization: ECSS-E-ST-10-03C, 2012
European Cooperation for Space Standardization: ECSS-Q-ST-70-04C, 2008

Jméno a pracoviště vedoucí(ho) diplomové práce:

Ing. Jaromír Kučera, ústav letadlové techniky FS

Jméno a pracoviště druhé(ho) vedoucí(ho) nebo konzultanta(ky) diplomové práce:

Datum zadání diplomové práce: **30.10.2020**

Termín odevzdání diplomové práce: **15.01.2021**

Platnost zadání diplomové práce: _____

Ing. Jaromír Kučera
podpis vedoucí(ho) práce

Ing. Robert Theiner, Ph.D.
podpis vedoucí(ho) ústavu/katedry

prof. Ing. Michael Valášek, DrSc.
podpis děkana(ky)

III. PŘEVZETÍ ZADÁNÍ

Diplomant bere na vědomí, že je povinen vypracovat diplomovou práci samostatně, bez cizí pomoci, s výjimkou poskytnutých konzultací. Seznam použité literatury, jiných pramenů a jmen konzultantů je třeba uvést v diplomové práci.

Datum převzetí zadání

Podpis studenta

Declaration

I declare that this thesis on the subject *Validation of Temperatures in a Thermal-Vacuum Chamber* is my own and has been written by me as the result of my own research under the supervision of Ing. Jaromír Kučera using literature listed at the end.

Prague 11. 01. 2021

.....
Matěj Koubek

Acknowledgements

I would like to thank my supervisor, Ing. Jaromír Kučera, whose valuable guidance provided me the support necessary to complete my thesis.

In addition, I would also like to thank my colleague Ing. Ondřej Šantora for his counsel and insightful feedback.

Abstract

This Master's thesis analyzes the systems of Thermal-Vacuum Chambers and types of tests they are used for. Results of the research are used to design a simulation of Thermal Cycling which are then validated using experimentally measured data.

Keywords: Thermal-Vacuum Chamber, Thermal Cycling, Simulation

Anotace

Obsahem této diplomové práce je řešení systémů Termovakuových komor a testů v nich prováděných a využití získaných poznatků k provedení simulace termálního cyklování. Práce je zakončena validací simulace pomocí experimentálně naměřených hodnot.

Klíčová slova: Termovakuová komora, Termální cyklování, Simulace

Contents

1	Introduction	1
2	Space Thermal and Vacuum Environment	
	Simulation Chambers	2
2.1	Space Environment	2
2.2	Thermal tests	3
2.3	Test Levels	3
2.4	Baselines, Requirements, and Standards	4
2.5	Simulation of Space environment	6
2.5.1	Test Equipment	6
2.5.2	Thermal Environment Simulation	8
2.5.3	Pressure Environment Simulation	8
2.5.4	Solar Environment Simulation	10
2.6	Other Systems of Thermal and Vacuum Simulation Chambers	10
2.6.1	Pressure measurement	10
2.6.2	Contamination measurement	12
2.6.3	Venting System	12
3	Simulation Tools and Methods	13
3.1	Mathematical modelling	13
3.1.1	CAD Model and Software	14
3.1.2	Discretization	14
3.1.3	Finite Element Analysis and Computational Fluid Dynamics	14
3.1.4	Boundary Conditions	16
3.2	Governing Equations of Thermal-flow Mathematical Model	17
3.2.1	Flow	17
3.2.2	Heat transfer - Conduction	17
3.2.3	Heat transfer - Convection	17
3.2.4	Heat transfer - Radiation	17
4	Details of Validation Experiment	18
4.1	Sensor Placement	18
4.2	Experiment Profile	19
4.3	Experiment Results	19

5	Simulation Setup	20
5.1	Model Assembly	20
5.2	Mesh Generation	21
5.3	Solution Parameters	23
5.4	Incorporation of Boundary Conditions	24
5.5	Simulation Results	27
6	Evaluation of Results	29
6.1	Nodal Temperature over Time	29
6.2	Deviation from Experiment	32
6.3	Interpretation of Results	34
6.3.1	Heating Phase	34
6.3.2	Dwell Phase	34
6.3.3	Cooling Phase	34
7	Conclusion	35
	List of symbols	36

1 Introduction

In this Master's thesis I am creating a thermal simulation of gaseous nitrogen flowing through a cold plate.

The simulation parameters portray a real-life scenario of an existing Thermal-Vacuum Chamber located in CTU laboratory in Prague. The simulation's design criteria are: the dimensions of the Thermal-Vacuum chamber, the flow rate of gaseous nitrogen, the materials used for the cold plate, the heat radiated from the Thermal shroud, and the ambient conditions during the experimental verification.

The thesis includes research on Thermal-Vacuum Chambers and Simulation Tools with the capability to simulate within the operational parameters of Thermal-Vacuum Chambers.

The goal of the thesis is to design a simulation that can be used for future pre-experiment simulations. Such an outcome has the potential to give beneficial insight into the experiment and may reveal problems that would otherwise be costly and time-consuming. For the simulation to be successful all temperatures, for points that would come in contact with a tested subject, should be within 20°C from their experimental counterparts.

2 Space Thermal and Vacuum Environment Simulation Chambers

When developing a spacecraft for applications in space such as communications, weather observation, navigation, planetary exploration, and others, it is important to have all the systems and subsystems tested and validated for the environment they will be subjected to. The reason for all these tests is that the cost of failure may be extremely high due to the loss of mission capability and the loss of equipment. Specifically for spacecraft, the main environmental sources of concern and therefore most important environmental tests include acoustic tests, thermal tests, vacuum tests, and vibration tests in no particular order. In this research, I will be focusing on the combination of thermal and vacuum testing. [1, 2, 3]

2.1 Space Environment

The ambient environment of a spacecraft strongly depends on its orbit. However, some characteristics remain constant: high vacuum, cold space environment, and radiation from different sources. These characteristics are shown in Table 1 and Figure 2.1.

Pressure	$0.1 - 1 \cdot 10^{-10} Pa$
Temperature	$3 - 4 K$
Solar flux	$1373 W/m^2$
Albedo radiation	$480 W/m^2$
Earth's radiation	$230 W/m^2$

Table 1: Space Environment in proximity to Earth [4]

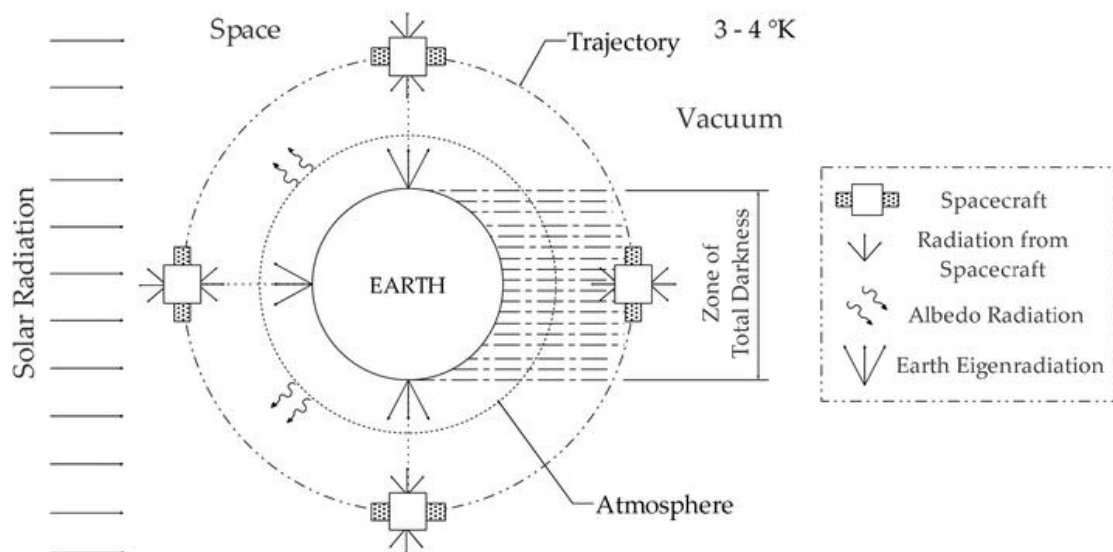


Figure 2.1: Space Environment in proximity to Earth [5]

2.2 Thermal tests

In order to validate any part of a spacecraft, several types of thermal tests must be performed. These tests ensure spacecraft's survivability and unhindered performance in the environment of deep space. They are as follows:

- **Thermal Cycle Test (TCT):** The test subject is exposed to a hot and cold temperature cycle at ambient pressure to identify material defects.
- **Thermal Vacuum Cycling Test (TVCT):** The test subject is exposed to a hot and cold temperature cycle in a high vacuum environment to verify the functionality of systems and subsystems.
- **Thermal Balance Test (TBT):** The test subject's thermal deformations are measured and its ability to maintain operational temperatures demonstrated.
- **Bake-out Test:** The test subject is exposed to a high temperature in a high vacuum environment to assess its outgassing.

The number of thermal cycles, temperature range, and other parameters are dependent on the type of test level. [6]

2.3 Test Levels

The beforementioned tests are performed at various temperatures each accomplishing a different goal.

- **Development Tests:** Not specified in any standard. Mainly to point out any flaws in the system's design that would otherwise be unnoticed until Qualification Tests.
- **Qualification Tests:** A formal proof that the design meets all the requirements of the specification and the parameters agreed with adequate margin, including manufacturing imperfections. Performed at temperatures harsher than what is to be expected during a mission for that particular test subject. Parts tested this way are not considered for the flight.
- **Acceptance Tests:** A formal proof that the product is free of workmanship defects and meets performance requirements with adequate margin. Performed at temperatures no more severe than those expected during the course of the mission.
- **Proto-Qualification Tests:** Another strategy of testing. Temperature levels are generally between those for Qualification and Acceptance Tests. Consists of testing first hardware to Proto-Qualification requirements to verify the design and testing

subsequent hardware to a level of Acceptance Tests for workmanship defects. Unlike units tested at the level of Qualification Tests, this first Proto-Qualification Tested unit is flight-worthy.

Test Levels are chosen according to the followed Standard. [6, 7]

2.4 Baselines, Requirements, and Standards

Any test must be done within some chosen specifications to enable comparison between similar test subjects. In this section, I will go into all the different standards that describe their own testing requirements to validate spacecraft, systems, or subsystems for a given purpose. Following handbooks were created by NASA, ESA, and the USA's Department of Defense. Comparison of the presented standards is shown in Table 2 below.

- **GSFC-STD-7000:** Standard that provides requirements and guidelines for environmental verification for payloads, subsystems, and components. It also elaborates on those requirements, gives guideline test levels, provides guidance in the choice of test options, and describes acceptable test and analytical methods for implementing the requirements. [8]
- **MIL-STD-1540D:** This document is intended for use in developing the detailed verification requirements for a particular project. The application of these requirements should result in an effective verification process and consequently high confidence in achieving successful space missions. This standard does not describe any value for any test. However, it suggests referring to MIL-HDBK-340A for testing requirements. [3]
- **MIL-HDBK-340A:** This handbook provides guidance for establishing uniform procedures for the control, determination, and documentation of product verification test requirements for launch, upper-stage, and space vehicles. [9]
- **ECSS-E-ST-10-03C:** This standard describes the requirement for performing verification by testing of spacecraft. It also states that a thermal vacuum test shall be performed for any equipment or spacecraft that is expected to operate under a vacuum environment. [10]
- **TR-2004(8583)-1 Rev.A.:** This standard establishes the environmental testing requirements for launch vehicles, upper-stage vehicles, space vehicles, and their subsystems and units. The test requirements herein focus on design verification and the identification of latent defects to help ensure a high level of confidence in achieving successful space missions. [11]

		GSFC-STD-7000	MIL-HDBK-340A	ECSS-E-ST-10-03C	TR-2004 (8583)-1 Rev.A.
Qualification	Chamber pressure	$1.33 \cdot 10^{-3} Pa$	$13.3 \cdot 10^{-3} Pa$	$10^{-3} Pa$	$13.3 \cdot 10^{-3} Pa$
	Temp. margins*	$10^{\circ}C$	No info	<i>See^f</i>	$10^{\circ}C$
	Number of cycles	4	13^a or 3^b	4	8
	Dwell time	24h	$8h^c$ or $4h^d$	No info	$8h^c$ or $4h^d$
Acceptance	Chamber pressure	No info	$13.3 \cdot 10^{-3} Pa$	$10^{-3} Pa$	$13.3 \cdot 10^{-3} Pa$
	Temp. margins*	$5^{\circ}C$	No info	<i>See^g</i>	$0^{\circ}C$
	Number of cycles	No info	13^a or 3^b	3^e	4
	Dwell time	No info	$8h^c$ or $4h^d$	No info	$8h^c$ or $4h^d$
Proto-Qualification	Chamber pressure	No info	No info	$10^{-3} Pa$	$13.3 \cdot 10^{-3} Pa$
	Temp. margins*	No info	No info	<i>See^f</i>	$5^{\circ}C$
	Number of cycles	No info	No info	3^e	4
	Dwell time	No info	No info	No info	$8h^c$ or $4h^d$
Tolerances	Pressure	$\pm 80\%$	$\pm 80\%$	$\pm 80\%$	0/ - 80%
	Temperature	$\pm 2^{\circ}C$	$\pm 3^{\circ}C$	$\pm 4^{\circ}C$	$\pm 3^{\circ}C$

Table 2: Comparison between rules and standards [6]

*These temperature margins are with respect to the worst expected temperatures

^aIf no thermal cycling test was performed before

^bIf thermal cycling test was performed before

^cFirst and last thermal cycles

^dIntermediate cycles

^ePlus one back up cycle that can be decided to be performed during tests

^fQualification and proto-qualification temperature limits are reached when any equipment reaches its qualification temperature limits. Its qualification limits represent the maximum and minimum acceptance temperatures and a $5^{\circ}C$ margin.

^gAcceptance temperature limits are reached when any equipment reaches its qualification temperature limits. Its qualification limits represent the maximum and minimum design temperatures and a $5^{\circ}C$ margin.

2.5 Simulation of Space environment

2.5.1 Test Equipment

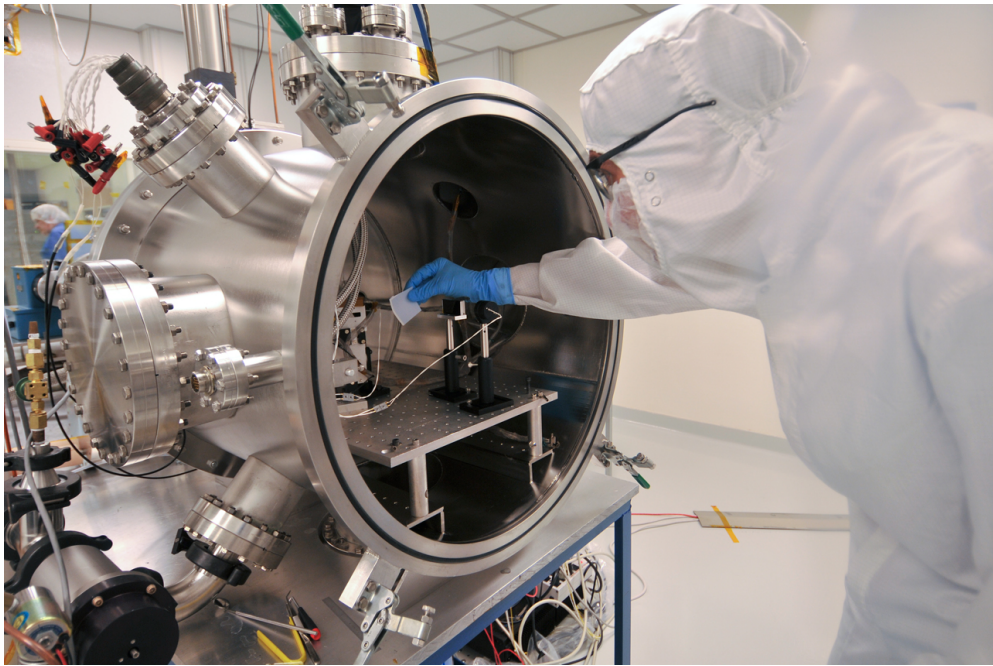
The devices used for space environment testing are called Thermal Vacuum Chambers and Space Simulation Chambers. Their purpose is to recreate the conditions that a spacecraft will experience in space as close as possible. One of their key functions is creating pressure low enough, to preclude thermal convection. Data gathered is used for spacecraft, subsystem, and component Qualification and Acceptance. They consist of vacuum pumps, means for cooling and heating, and in the case of Space Simulation Chambers, they also include a source of radiation. [12]

The best way to differentiate between Thermal-Vacuum Chambers (fig 2.2a) and Space Simulators (fig 2.2b) is the method of temperature regulation inside the chamber. While Thermal-Vacuum Chambers take the easier approach and heat/cool the test subject by conduction through a plate the said object is mounted to, the Space Simulation Chambers use hot/cold gas propelled through a shroud changing the temperature of the subject through the manner of radiation. It needs to be noted that this is the approach most widely used and is in no way unchangeable. Overlooking the inner components of the chamber, available options for thermal control of the medium are shown in Table 3.

Medium	Cooling	Heating	Temperature Range
LN_2	Flooding / Circulation	None	$-185^\circ C$ only
LN_2	Flooding / Circulation	Resistance Heating	$-185^\circ C$ to $+150^\circ C$
GN_2	LN_2 Injection	Electric in Conditioner	$-185^\circ C$ to $+150^\circ C$
GN_2	LN_2 Exchanger	Electric in Conditioner	$-170^\circ C$ to $+150^\circ C$
GN_2	Mechanical Cooling	Electric in Conditioner	$-70^\circ C$ to $+150^\circ C$
Coolant*	LN_2 Exchanger	Electric in Conditioner	$-85^\circ C$ to $+150^\circ C$
Coolant*	Mechanical Cooling	Electric in Conditioner	$-85^\circ C$ to $+150^\circ C$

Table 3: List of Thermal Conditioning Options [13]

*Available coolants include: d-Limonene, Propylene Glykol, FC77 Flourinert, Galden HT170, Lexol 408, Paratherm CR, Coolanol 25, etc. Temperature ranges differ with each coolant and can be acquired from their manufacturer.



(a) LASP Vacuum Test Chamber [14]



(b) TriasRnD Space Simulation Chamber [15]

Figure 2.2: Examples of Simulation Chambers

2.5.2 Thermal Environment Simulation

Simulating space thermal environment with close proximity would be economically unviable, therefore through analysis of previous data and utilization of Stefan-Boltzmann law the optimal temperature range with acceptably small error percentage was set between $77 - 100K$.

To reach this temperature a thermal system consisting of a thermal shroud and a thermal plate is used. A Thermal shroud is a surface between the test subject and the inner part of the chamber. Covered by a finish with a high absorption coefficient to simulate the Space radiation background. The shroud has an inner pipeline structure usually filled with cryogenic liquids to absorb all the heat radiated from the test subject.

The thermal plate is a surface to which the test subject is installed to. This plate is cooled the same way, but it absorbs heat through conduction instead of radiation. For this reason, these plates are usually made from aluminium alloys with high thermal conductivity and strength.

To get to the other side of the spectrum several heating methods can be used. The simplest one is an electrical heater embedded inside of the thermal plate, others include infrared heaters, hot gas heating the thermal shroud, or tubular heaters such as Watrods. [16, 17]

2.5.3 Pressure Environment Simulation

To achieve a specific level of vacuum (dependent on the predicted conditions of the test subject's orbit) a pumping system is required. This system usually consists of two and possibly more pumps, each operating in a different pressure range. The pumping process can be divided into two parts: roughing and backing. One being from ambient pressure to 0.1 Pa while the second one goes from 0.1 Pa to the highest vacuum the pump is capable of. Vacuum Pumps and their capabilities are shown in Table 4. It needs to be pointed out that the pumps most used are the Rotary plunger, Cryopump (fig 2.3a), Scroll pump (fig 2.3b), Turbomolecular Pump (fig 2.3c), and Adsorption pump in no particular order.

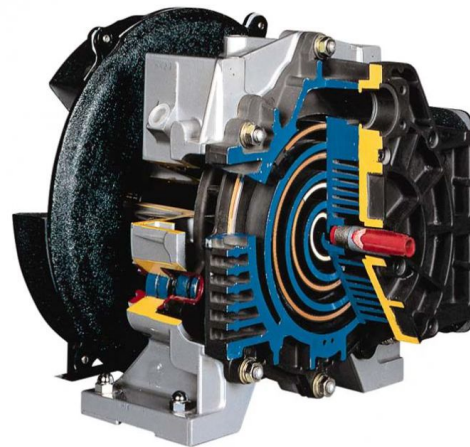
The quality of the vacuum is dependent on factors such as the type of a vacuum pump, rate of outgassing from chamber elements, conductance in lines, and cleanliness of the pump system. The pump type is important because some types use oil for cooling or vacuum generation itself. This oil may turn into vapour and represent a risk of polluting the chamber. This risk can be mitigated with the use of cold traps.

Said trap is installed in the path of the pumped gases outside the vacuum chamber. It uses cryogenic liquids to generate low temperature and crystalize gas molecules that impact its surface effectively reducing amount of oil vapour and speeding up the whole process. This process is called deposition and the same principle can be applied inside the chamber as well. Such devices are called decontamination plates or cold plates. [4]

2.5 Simulation of Space environment



(a) Cryogenic Pump [18]



(b) Scroll Pump [19]



(c) Turbomolecular Pump [20]



(d) Diffusion Pump [20]

Figure 2.3: Examples of Vacuum Pumps

Vacuum Pump	Pressure range
Piston	$10^5 Pa - 10^3 Pa$
Diaphragm	$10^5 Pa - 10^3 Pa$
Trochoide	$10^5 Pa - 10^1 Pa$
Liquid jet	$10^5 Pa - 10^1 Pa$
Scroll	$10^5 Pa - 10^0 Pa$
Adsorption	$10^5 Pa - 10^{-1} Pa$
Sliding-vane rotary	$10^5 Pa - 10^{-1} Pa$
Rotary plunger	$10^5 Pa - 10^{-1} Pa$
Roots	$10^5 Pa - 10^{-1} Pa$
Vapor jet	$10^4 Pa - 10^{-1} Pa$
Diffusion ejector	$10^4 Pa - 10^{-4} Pa$
Diffusion	$10^{-1} Pa - 10^{-5} Pa$
Turbomolecular	$10^{-1} Pa - 10^{-8} Pa$
Sublimation	$10^{-2} Pa - 10^{-8} Pa$
Sputter-ion	$10^{-2} Pa - 10^{-9} Pa$
Cryopump	$10^{-2} Pa - 10^{-9} Pa$

Table 4: Working ranges of vacuum pumps [21]

2.5.4 Solar Environment Simulation

The last main environmental element is solar radiation. This is where Thermal Vacuum Chambers and Space Simulation Chambers differ. While Thermal Vacuum Chambers simulate only pressure and thermal cycling, the Space Simulation Chambers are designed to simulate solar radiation as well.

This radiation is simulated by a system of lamps and lenses. Lamps used are usually Xenon (fig 2.4a) or Carbon-Arc with the flux of at least $1.35 kW m^{-2}$. The heat produced by these lamps is offset by a cooling system of some sort. A diagram of such a system (albeit not from a Vacuum Chamber) is shown in Figure 2.4b. Chambers of this type can also include a motion simulator to orient the test subject with respect to the light beam. [22]

2.6 Other Systems of Thermal and Vacuum Simulation Chambers

2.6.1 Pressure measurement

With the choice of vacuum pump comes the choice of a pressure gauge. Total pressure gauges are classified by the different ranges of vacuum they can measure and their internal mechanisms. A selection of total pressure gauges and their ranges are in Table 5. Some of the mechanisms include using the hydrostatic pressure, change of capacitance, or thermal conductivity. Sufficient calibration of the used gauge is vital to detect chamber

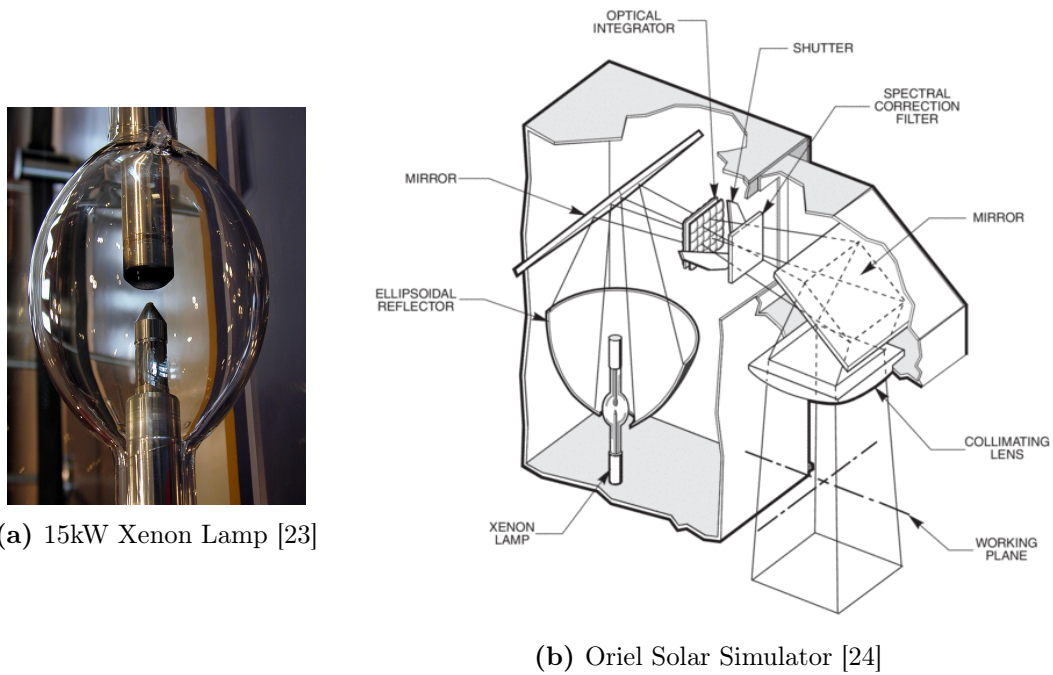


Figure 2.4: Solar Environment Simulation Technology

pressure correctly. For the purposes of Thermal-Vacuum Chambers, the best gauges to use are Penning gauge, the combination of Pirani and Convection gauges, Capacitance Manometer, and B-A ionization gauge (fig 2.5) in no particular order. [4]

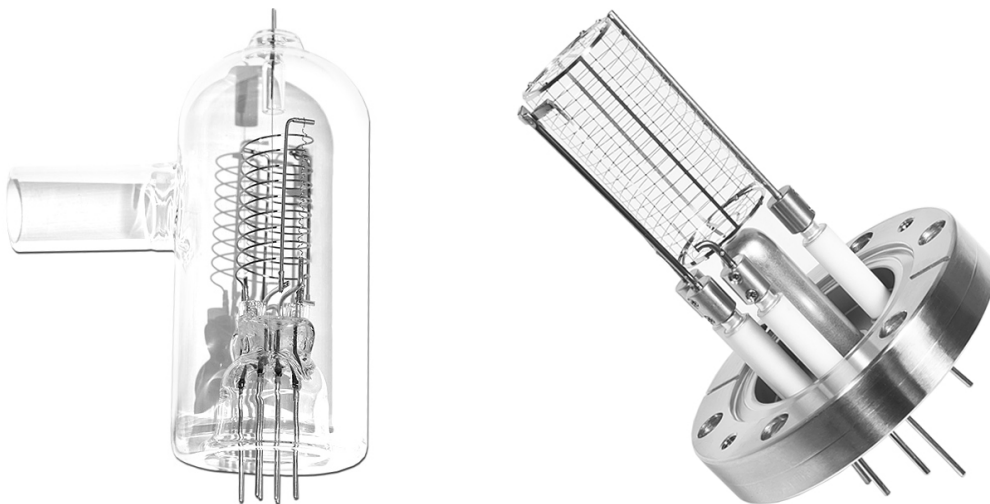


Figure 2.5: Bayard-Alpert Ion Gauges [18]

Pressure gauge	Pressure range
U-Tube manometer	$10^5 Pa - 10^2 Pa$
Diaphragm	$10^5 Pa - 10^2 Pa$
Pirani + convection	$10^5 Pa - 10^{-1} Pa$
Capacitance Manometer	$10^5 Pa - 10^{-4} Pa$
Thermocouple	$10^3 Pa - 10^{-1} Pa$
Pirani	$10^3 Pa - 10^{-1} Pa$
McLeod	$10^3 Pa - 10^{-1} Pa$
Penning	$10^{-1} Pa - 10^{-5} Pa$
B-A ionization	$10^{-1} Pa - 10^{-9} Pa$
Module BAG	$10^{-1} Pa - 10^{-9} Pa$
Extractor	$10^{-1} Pa - 10^{-10} Pa$
Quadrupole	$10^{-1} Pa - 10^{-12} Pa$
Inverted Magnetron	$10^{-2} Pa - 10^{-9} Pa$

Table 5: Working ranges of vacuum gauges [25]

2.6.2 Contamination measurement

Methods to measure contaminants are divided into direct and indirect. The direct methods are using a plate or a reflective material that is placed inside the chamber and analysed with residual gas analysers, mass spectrometers, or other techniques during operation. An indirect method happens after the thermal vacuum test finishes. The plate is removed from the chamber, cleaned and the resulting film is analysed with spectrometers. Techniques used for contaminant analysis include residual gas analysis, gas chromatography, infrared spectroscopy, and ultraviolet reflectance. [26]

2.6.3 Venting System

When all testing concludes and a vacuum is no longer required, the vacuum system activates a circuit that increases pressure by introducing a filtered dry inert gas into the chamber. It is important to control the rate of pressure increase to ensure safety. Inert gas is often used instead of air, because air (or other unfit gases) could react with the system's temperature and introduce water vapour molecules, contaminating the test subject and the chamber itself. [4]

3 Simulation Tools and Methods

Considering the scope of this field this section only contains the information necessary to solve problems presented in this thesis making it limited solely for this purpose.

The cooling process simulated in this thesis can be solved using two branches of physics. First is fluid dynamics, a discipline that describes the flow of fluids – liquids and gases. It is critical to know the speed and density of the liquid nitrogen that is pumped into the system. The second is thermodynamics. As the liquid nitrogen flows through the system it receives heat from its surroundings. In the beginning, it is heated up by the pipes between the reservoir and the cooling plate, after that it receives energy from both the aluminium frame and the aluminium shield. In the meantime, this aluminium subsystem is receiving energy in the form of electromagnetic waves from the inner cylindrical walls of the chamber.

There are all three types of heat transfer present. In the aluminium subsystem, the heat is exchanged through the means of conduction as the parts are solid and touching. Amidst the nitrogen and the aluminium subsystem, the heat is transferred by convection as the nitrogen is a fluid flowing past the solid aluminium parts. Lastly, the inner chamber walls irradiate the surface of said aluminium and vice versa. Considering the plate is being cooled by highly subfreezing temperatures and the chamber walls are heated by its surroundings it is safe to assume the plate will be receiving more heat than it gives off. It is worth mentioning that convection between air and the aluminium cooling system is negligible because the chamber operates in near-vacuum conditions making the energy transferred this way minimal.

3.1 Mathematical modelling

First, we should start with a definition of a mathematical model.

“A model is a set of mathematical equations that provide an adequate description of a physical system.” Rutherford Aris

“A physical system” can be broadly interpreted as any real-world problem – natural or man-made, discrete or continuous, deterministic or random in behaviour. Being “adequate” sometimes suggests having a minimal level of quality, but in the context of modelling, it describes equations that are good enough to provide sufficiently accurate predictions of the properties of interest without being too difficult to evaluate. In other words, a model is a useful, practical description of a real-world problem, capable of providing systematic mathematical predictions of selected properties.

Once a well-defined mathematical problem is set up, its mathematical study can be an important step in understanding the original problem. However, even when the model does not work as expected, it can lead to a better understanding of which parameters have a significant influence on the system’s behaviour and how to further improve the

accuracy of the model. Moreover, simple, approximate solutions are more useful than complex exact solutions so trying to include every possible effect would be counterproductive as the computing times get significantly higher and the odds of a converging solution diminish. [27]

3.1.1 CAD Model and Software

Parameters influencing the choice of software are as follows. For simplicity's sake, the program needs to be able to both make a model of the Thermal-Vacuum Chamber and all its subsystems and to apply chosen transient Finite Element Analysis and present a solution. It needs to solve thermal changes in both solids and liquids while considering nitrogen flow. Furthermore, radiative heat exchange with the environment must be considered. For all those reasons mentioned the software chosen is Siemens NX with Simcenter 3D Thermal/Flow Solver.

When the problem in question is well understood a Computer Aided Design Model can be developed. In this case, it contains the steel chamber, aluminium cooling system, and support beams. Because these parts were manufactured corresponding drawings provide all information necessary. The model and a photo of the CTU owned chamber is shown in Figure 3.1.

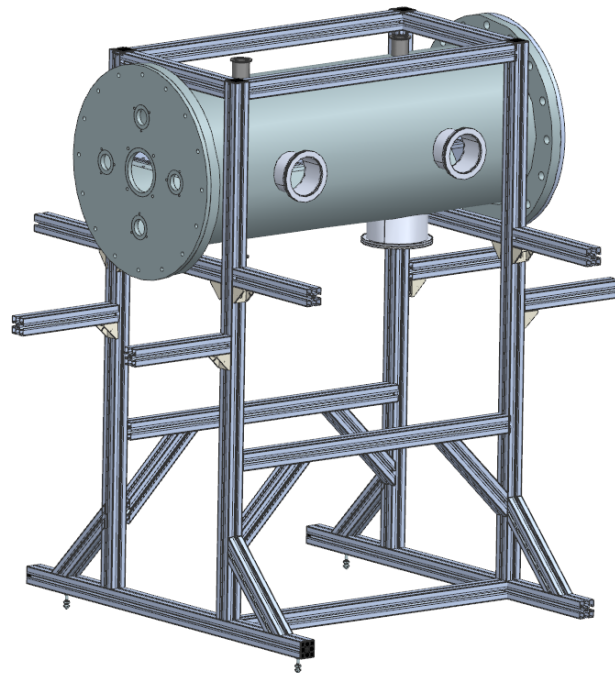
3.1.2 Discretization

Discretization is a mathematical process of transferring continuous parameters into discrete counterparts. It is a necessary alteration of the computing environment to make the application of differential equations in said environment possible. The point density of the newly discrete environment is directly proportional to the rate of change of a given variable. Connecting these points establishes a network called "Mesh".

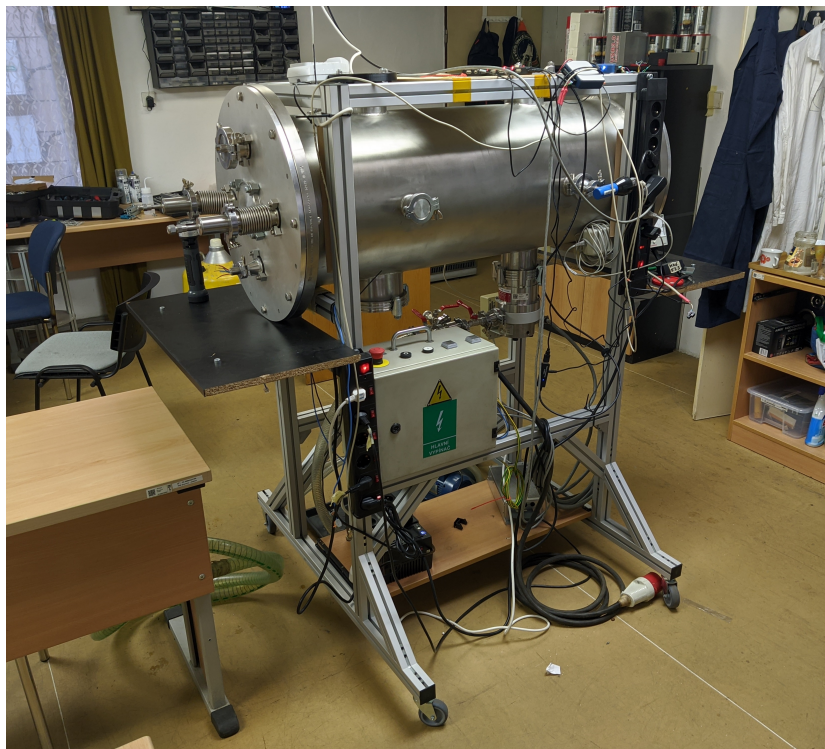
In a 3D space, this mesh consists of 4 different shaped cell types – Tetrahedron, pyramid, triangular prism, hexahedron. Selecting the right type and size of cells is vital to achieving relevant results in the shortest possible time.

3.1.3 Finite Element Analysis and Computational Fluid Dynamics

FEA and CFD both simulate a mathematical model. The difference between them is that FEA focuses on structural analysis (including thermal analysis) while CFD is focused on fluid dynamics. Combining these two makes the problem presented in this thesis solvable. During the simulation, calculations run for every point in the mesh while interpolations occur between them. The equations the model solves for are listed in Section 3.2.



(a) NX Model



(b) Photo During Operation

Figure 3.1: CTU Thermal-Vacuum Chamber

3.1.4 Boundary Conditions

The main mechanism to designate a solution is the introduction of boundary conditions. They are the constraints necessary to solve a given set of differential equations in the rest of the mesh. There are several types of boundary conditions named after scientists that first presented them (Dirichlet boundary condition, Neumann boundary condition, etc.) and have different applications depending on simulation type. Presented boundary conditions are derived from experimental conditions of CTU's Thermal-Vacuum chamber, which has a cold plate thermally regulated by liquid nitrogen and heating foil.

- **Ambient temperature:** The Thermal-Vacuum Chamber itself is located in a room with a temperature stable enough to call it fixed.
- **Initial temperature:** Thermal cycle is simulated in two parts, the heating portion, and the cooling portion. Meaning any simulation starts from either a heated or a cooled state. This state is a boundary condition for the coolant and the aluminium body and plates.
- **Flow inlet:** The flow of coolant through the cooling system must be defined. Either by its velocity, mass flow, pressure difference, etc.
- **Flow opening:** As the end of the cooling system's piping is just an opening for the inert gas to escape, this boundary condition is just a definition of temperature and pressure conditions beyond.
- **Flow surface:** This condition defines the interaction between the coolant and the aluminium body. It specifies both the heat and mechanical energy exchange.
- **Surface to surface contact:** Considering the solid parts of the cooling systems are touching, there must be heat exchange through the means of conduction happening. Using this, the details of the heat exchange can be adjusted to better reflect real-world conditions.
- **Joule heating:** For the heating part of the cycle a heating foil can be represented by this condition.
- **Radiation:** Per Stefan-Boltzmann's law both the inner wall of the chamber and the cooling system emits electromagnetic waves and their strength is determined by their temperature, area, and emissivity. That makes this boundary condition necessary.

One condition not mentioned is Convection to environment. The reason being, that because the chamber is depressurized, there are not enough molecules present to warrant its inclusion.

Proper incorporation of all abovementioned boundary conditions into a well-meshed model that represents a correctly defined problem should then lead to realistic results.

3.2 Governing Equations of Thermal-flow Mathematical Model

The governing equations of a mathematical model describe how the values of the unknown variables change when one or more of the known variables change. [28]

3.2.1 Flow

Fundamental equations defining flow are the Continuity Equation (3.1), the Equation of Motion derived from Newton's second law (3.2), and Navier-Stokes momentum equation for compressible flow (3.3). [29]

$$\frac{\delta \mathbf{u}_x}{\delta x} + \frac{\delta \mathbf{u}_y}{\delta y} + \frac{\delta \mathbf{u}_z}{\delta z} = 0 \quad (3.1)$$

$$\frac{\delta \mathbf{u}}{\delta t} + (\mathbf{u} \cdot \nabla) \mathbf{u} = \mathbf{g} + \frac{1}{\rho} \nabla \cdot \sigma_{ij} \quad (3.2)$$

$$\rho \frac{D\mathbf{u}}{Dt} = \rho \left(\frac{\delta \mathbf{u}}{\delta t} + \mathbf{u} \cdot \nabla \mathbf{u} \right) = -\nabla \bar{p} + \mu \nabla^2 \mathbf{u} + \frac{1}{3} \mu \nabla (\nabla \cdot \mathbf{u}) + \rho \mathbf{g} \quad (3.3)$$

3.2.2 Heat transfer - Conduction

Conduction is defined as the transfer of internal energy by microscopic collisions of molecules or other particles within a body. When two things touch, the faster-moving molecules of the warmer object crash into the slower moving molecules of the colder object giving them energy and increasing temperature. This transfer of energy is also known as Fourier's law (3.4).

$$\frac{\Delta Q}{\Delta t} = -k \cdot A \cdot \frac{\Delta T}{\Delta x} \quad (3.4)$$

3.2.3 Heat transfer - Convection

A mechanism of energy transfer by the physical movement of a fluid, which can be liquid or gas. This phenomenon can be described by equation 3.5.

$$\frac{\Delta Q}{\Delta t} = h_c \cdot A \cdot \Delta T \quad (3.5)$$

3.2.4 Heat transfer - Radiation

Thermal radiation refers to the process by which an object radiates its thermal energy in the form of electromagnetic waves. This process is described by the Stefan-Boltzmann law (3.6).

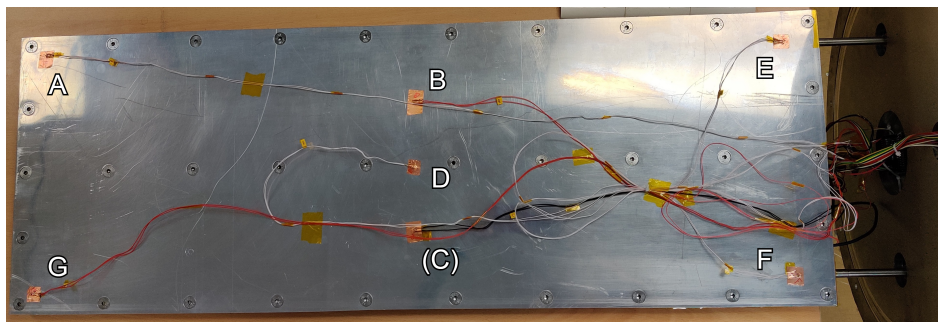
$$\frac{\Delta Q}{\Delta t} = e \cdot \delta \cdot A \cdot T^4 \quad (3.6)$$

4 Details of Validation Experiment

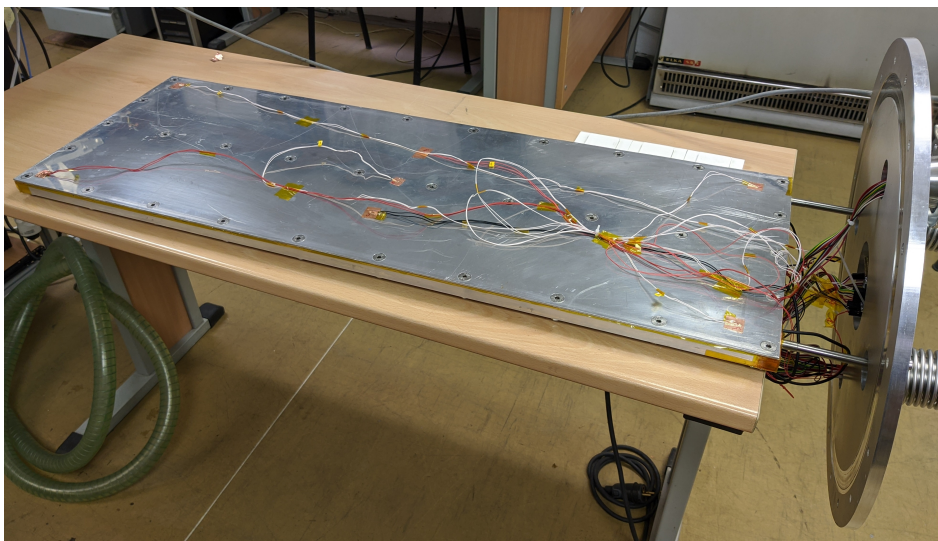
4.1 Sensor Placement

The experiment conducted to validate the simulation data consisted of temperature measurements from 7 key points on the top aluminium sheet, temperature measurements of nitrogen leaving the cooling subsystem, weight measurements of remaining nitrogen, and pressure measurements inside the chamber. Data regarding pressure is not presented in this thesis because their purpose was confirming the vacuum quality meets requirements presented in the beforementioned research.

Sensor positions were chosen as follows: above entry and exit tunnel, on both corners opposing the openings, centre of the plate, and in the middle of the second tunnel from the start. One more sensor was present, however, it was not secured correctly, therefore its data was neglected. The sensor in question was sensor "C". Their positions are shown in Figure 4.1 and in Attachment 2. The temperature of escaping gas was measured by a sensor inserted into the opening roughly under the plate exit sensor. The remaining nitrogen was logged by a scale and correlated with time to obtain mass flow.



(a) Sensor Placement



(b) Overview of Electronics

Figure 4.1: Thermal Control System Experiment Setup

4.2 Experiment Profile

After the chamber reached a pressure below $10^{-4} Pa$ the system was put through several thermal cycles. Firstly, heating the top plate to a temperature exceeding $80^{\circ}C$, waiting 10-15 minutes for the temperatures to even out, and then cooling the whole system down. Both the heating wattage and mass flow rate of nitrogen were altered throughout the experiment to acquire as wide data range as possible. The cycle with the most uniform heating and steadiest cooling was the one chosen as the simulation comparison.

4.3 Experiment Results

Details of the designated cycle are presented in Table 6 and its position in the entire experiment is shown in Figure 4.2.

hh:mm:ss	t [s]	Action	Average Temperature
16:06:44	0	Heating ON	$-69.2^{\circ}C$
17:17:24	4240	Heating OFF	$81.9^{\circ}C$
17:32:51	5167	Cooling ON	$75.4^{\circ}C$
19:01:44	10500	Cooling OFF	$9.2^{\circ}C$

Table 6: Experiment Cycle Details

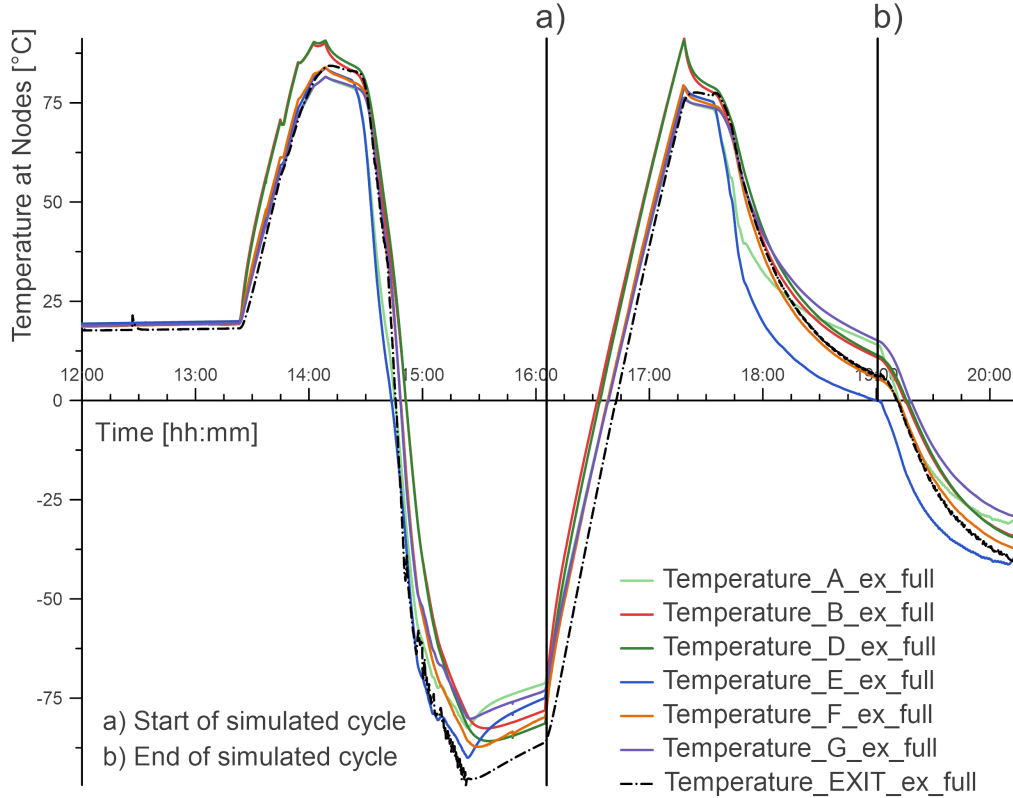


Figure 4.2: Temperature over Time - Full Experimental Data Set

5 Simulation Setup

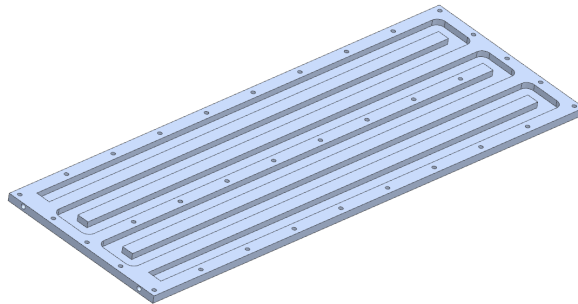
5.1 Model Assembly

The first part of the simulation setup is the assembly of necessary models. In this case, they are as follows: aluminium body (fig. 5.1a), negative of the groove containing nitrogen, aluminium sheets, and the steel walls of the chamber. In Figure 5.1b the negative and the two sheets are assembled to the main body. Lastly, this sub-assembly is situated inside the chamber (fig. 5.1c).

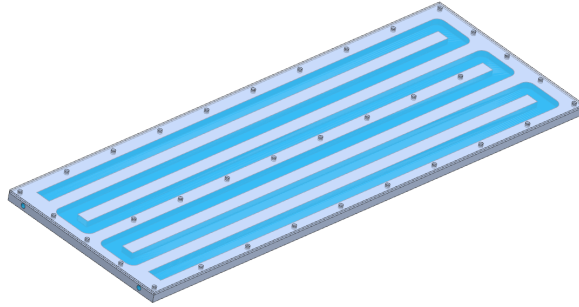
At this point, it is not necessary to add material properties to the solid bodies in the assembly as it will be done during the meshing process. It is, however, important to have the correct model dimensions and apply appropriate assembly constraints as it would otherwise invalidate the results of the simulation. In this case, both the dimensions and the assembly constraints correspond to reality and the main ones are listed in Table 7.

Main Body length	1000mm
Main Body width	350mm
Main Body thickness	15mm
Number of Aluminium Sheets	2
Aluminium Sheet thickness	3mm
Number of Ridges	6
Nitrogen Ridge length	950mm
Nitrogen Ridge width	30mm
Inner Chamber diameter	407mm
Inner Chamber length	1046mm
Position of Main Body	Centered

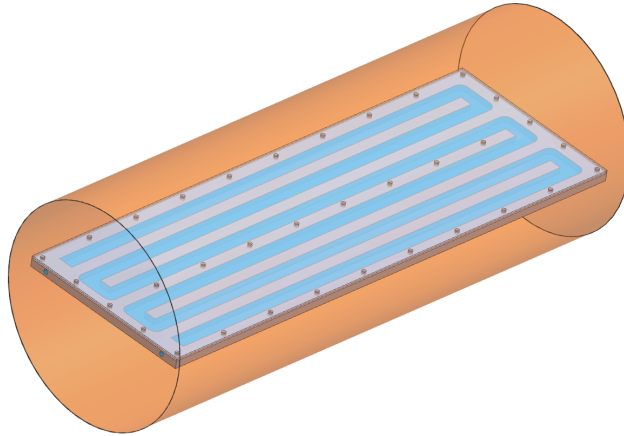
Table 7: Main Dimensions



(a) Model of the Aluminium Body



(b) Model including Aluminium Sheets



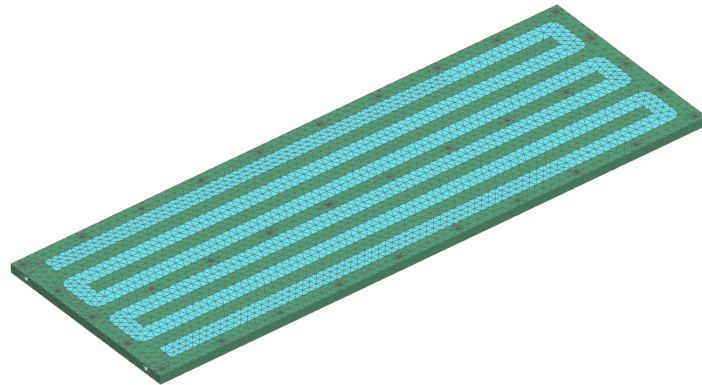
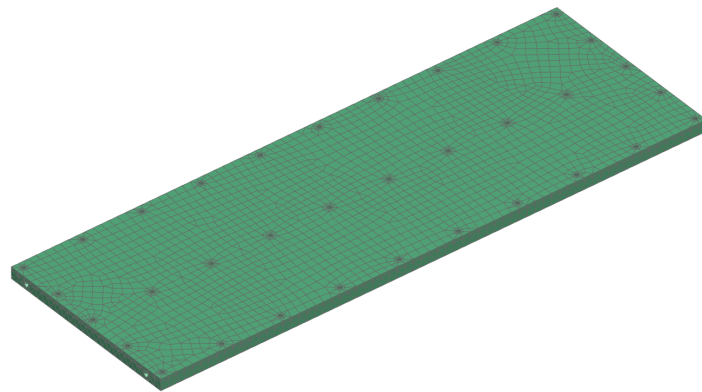
(c) Full Simulation Model

Figure 5.1: Model Assembly

5.2 Mesh Generation

The next part is the discretization of the models in the assembly. The finer the mesh, the higher the accuracy of the result. However, a nonlinear increase in computation time is expected. Meshing parameters are listed in Table 8 and final mesh examples are visualised in Figure 5.2. Chamber walls and gas inlet/outlet pipes are not included for reasons explained in Section 5.4.

Solid Body	Mesh Type	Element size
Main Body	3D Hybrid Mesh	15 mm
Aluminium Sheet	3D Swept Mesh	15 mm
Nitrogen Ridge	3D Tetrahedral Mesh	25 mm

Table 8: Mesh Parameters**(a)** Aluminium Body with Nitrogen Ridge Meshed**(b)** Full Simulation Model Meshed**Figure 5.2:** Examples of meshed parts

5.3 Solution Parameters

Choosing the right solver and adjusting its solution parameters determines which constraints and loads can be applied to the generated mesh. As mentioned in Section 3.1.1 the solver selected for this simulation is Simcenter 3D Thermal/Flow.

Analysis type, Solution type, and Main Solution Details are displayed in Figure 5.3. Other altered parameters are mainly related to the Transient Setup (Length of the Simulated Interval, Number of Time Steps in this Interval, and the Number of Results Sampled), and variables included in the Solution Report.

Following versions of the software were used: Siemens NX 1899; Simcenter 3D 2020.1.6

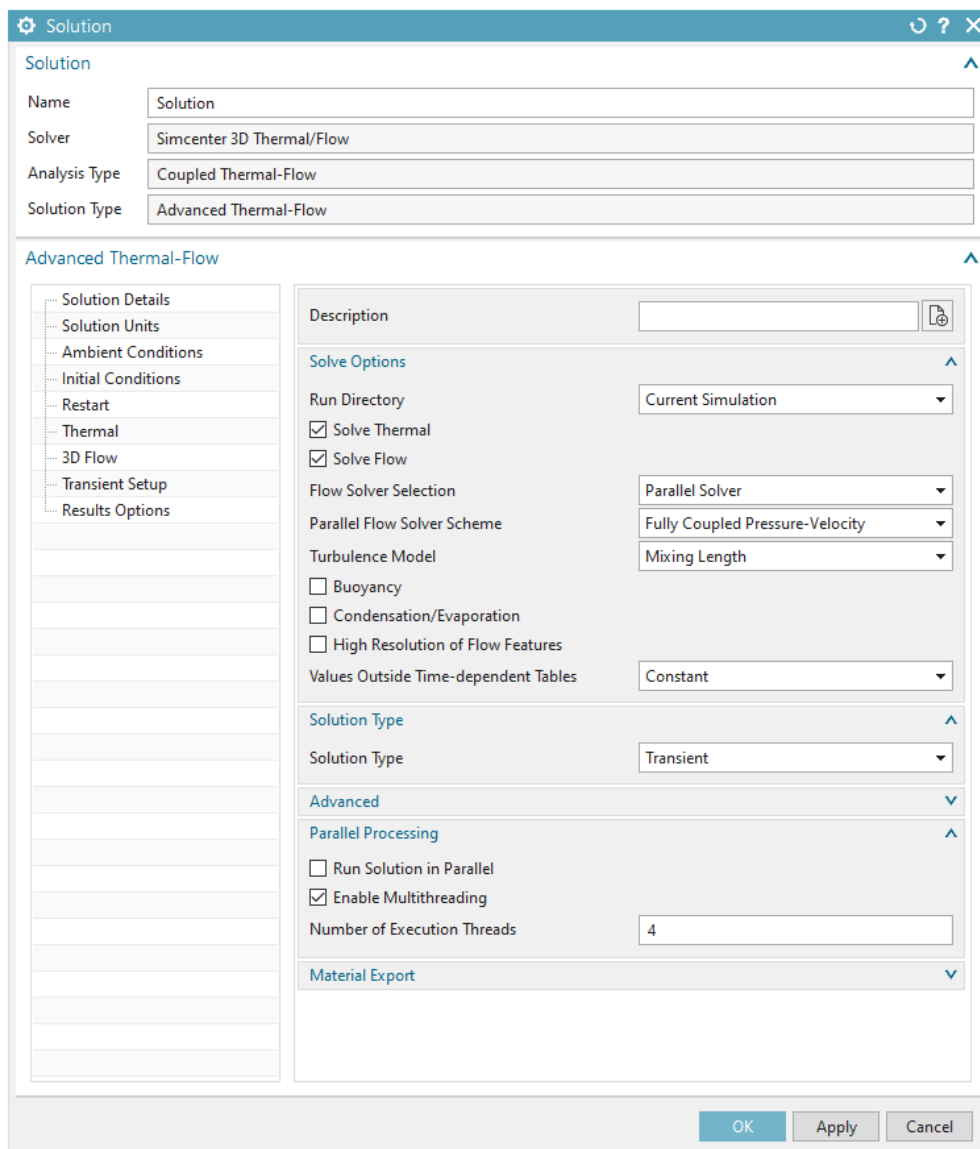


Figure 5.3: Solution Parameters

5.4 Incorporation of Boundary Conditions

Boundary conditions are used to simulate experimental conditions. The manner of their introduction defines the result. However, suitable adjustments to the real-life experiment can decrease computing time greatly while keeping the accuracy of the result satisfactory.

The main simplification applied to this simulation was the removal of radiation from the chamber walls and the addition of thermal load to the main cooling system surfaces. After testing, the thermal load determined by the Stefan-Boltzmann law was yielding comparable results, while decreasing the computation time of each time step by more than a half. This removes the necessity of meshing the chamber walls and the vacuum inside.

Another adjustment made was the exclusion of rounded edges inside the main body from heat transfer by convection. They were important to keep in the model because their removal would have a radical impact on flow, however, when solving the simulation with this type of heat transfer included, the software would crash. As the total area, these edges occupy is negligible compared to the rest of the ridge a solution is not necessary.

Bolts tightening the Thermal Control System were left out of the model because their size required much finer mesh compared to the rest of the assembly. Even though this decision introduced inaccuracies, the simulation time with their inclusion made the simulation unfeasible.

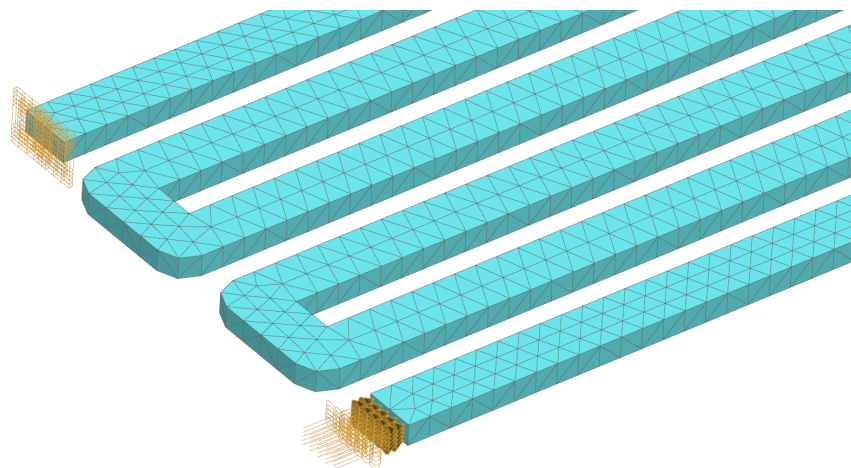
Final simplification is the position of the gas inlet/outlet. As there is minimal heat transfer in the small main body openings the simulation of flow starts in the rectangular cross-section. This adjustment decreased simulation time because the high-speed flow inside these openings was omitted.

"Flow inlet/outlet", "Flow surface", and "Radiation to environment" boundaries are visualised in Figure 5.4 and a complete list of applied boundary conditions is shown in Table 9.

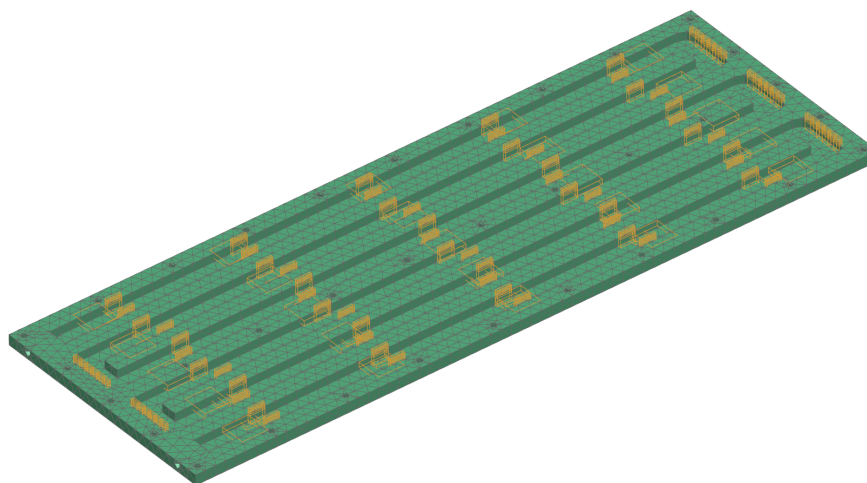
Flow Boundary Conditions - Cooling		
Inlet Flow Start*	Mass Flow	$6.2kg \cdot h^{-1}$
	External Conditions	$20^{\circ}C$
Inlet Flow after 600s*	Mass Flow	$6.2kg \cdot h^{-1}$
	External Conditions	$-195^{\circ}C$
Opening	External Pressure	$101,325Pa$
Surface to Surface Contact		
Between Al Sheets	Total Resistance	$0.01^{\circ}C/W$
Main Body and Al Sheet	Total Resistance	$0.001^{\circ}C/W$
Flow Surface		
Every Wetted Surface	No Slip Wall	Smooth with Friction
Initial Temperature Conditions		
Nitrogen Mesh		$-69.2^{\circ}C$
Every Solid Body		$-69.2^{\circ}C$
Radiation from Chamber Walls as Thermal Load		
Top and Bottom Surfaces	Heat Load	$45W$
Radiation to Environment		
Top and Bottom Surfaces	Emissivity	0.6
Heating Between Al Sheets		
Between Al Sheets	Thermal Load	$(26V \cdot 1.7A) \cdot 2$

Table 9: Boundary Conditions

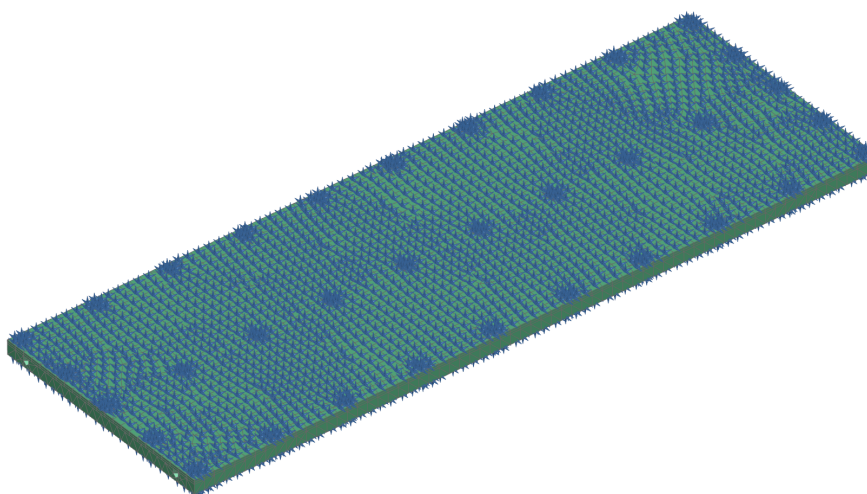
*Difference in initial gas temperature was included to account for the cooling of outside tubing. External Conditions of Inlet Flow between 0 and 600s were interpolated.



(a) Flow Inlet/Outlet Boundary Conditions



(b) Flow Surface Boundary Conditions



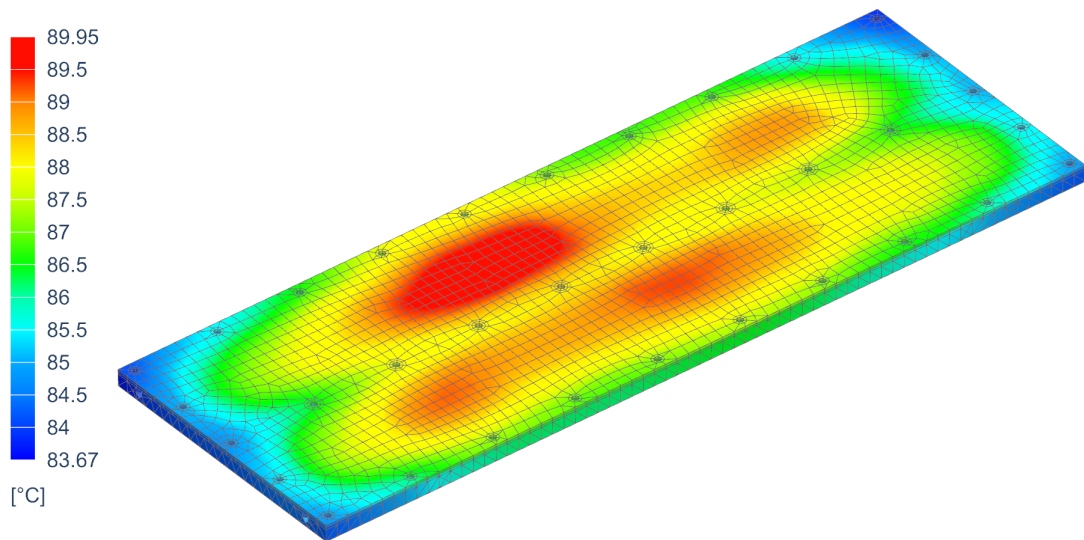
(c) Radiation to Environment Boundary Condition

Figure 5.4: Examples of used Boundary Conditions

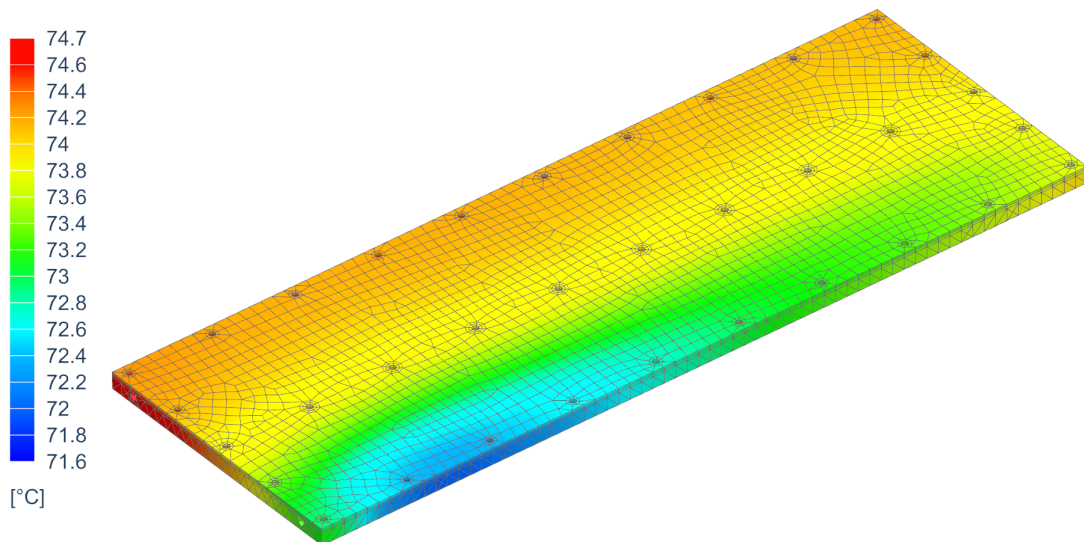
5.5 Simulation Results

Simulation parameters were adjusted to reflect the chosen experimental cycle and sensor positions were connected to corresponding mesh nodes.

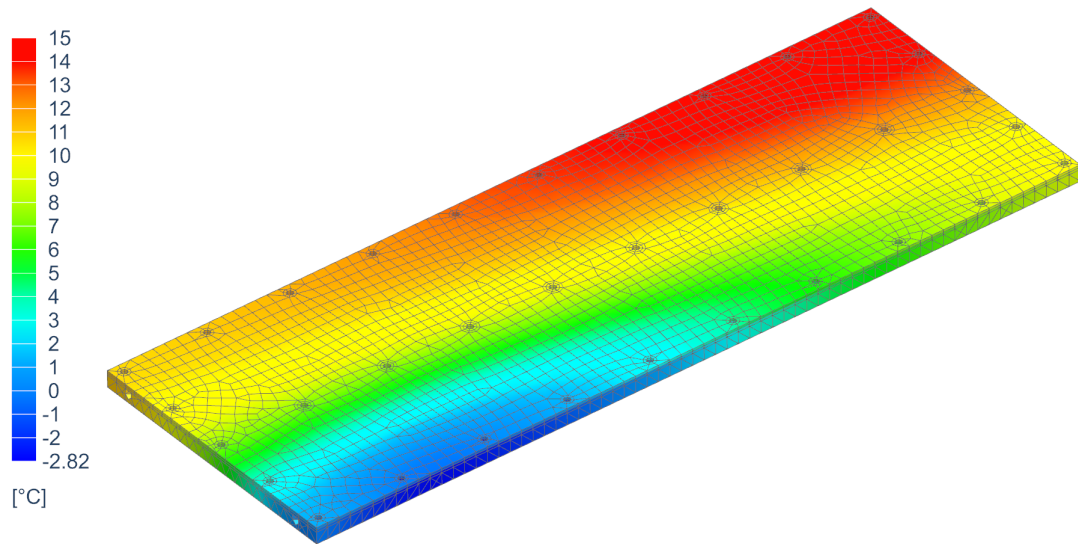
Following Contour Plots (fig. 5.5) show the Thermal Control System in 3 different stages of the simulation. Figure (a) shows Nodal Temperatures at the time the heating was switched off. Figure (b) shows Nodal Temperatures 90 seconds after cooling was switched on. Figure (c) and (d) both show the end of the simulation. Figure (c) contains the temperature of the Thermal Control System and Figure (d) the Elemental Temperature of the nitrogen inside it.



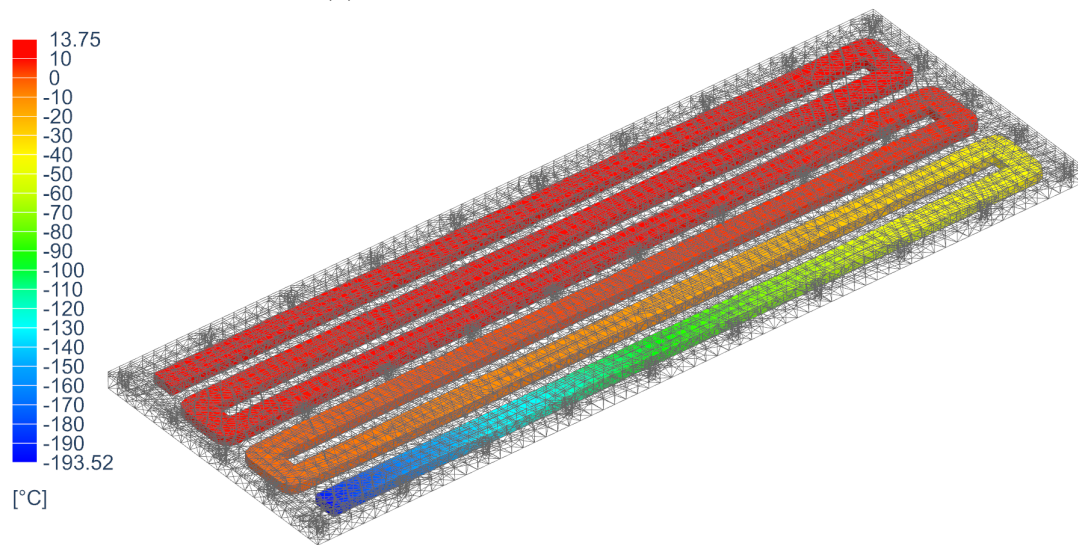
(a) Plate Temperature after Heating



(b) Plate Temperature after 90 seconds of Cooling



(c) Plate Temperature after Cooling



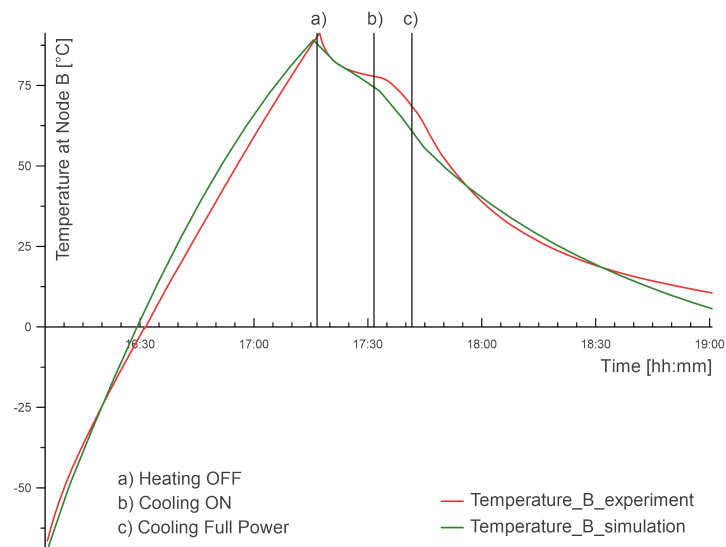
(d) Nitrogen Temperature at the end of Cooling Cycle

Figure 5.5: Simulation Results

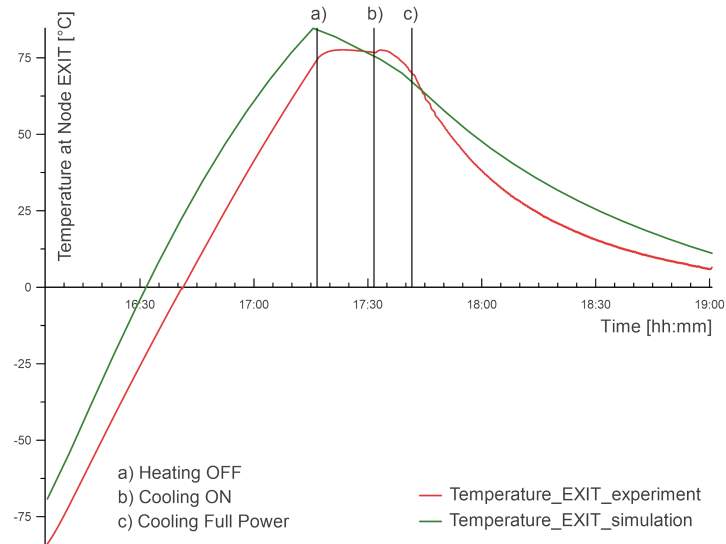
6 Evaluation of Results

6.1 Nodal Temperature over Time

Nodal data measured in the experiment was combined with the Mesh Point data computed in the simulation. For better clarity, the time frame used corresponds to the time frame of the experiment. Figure 6.1 shows temperature over time for Nodes that correlated the most (Node B) and the least (Node EXIT). Comparison of all Nodes is presented in Figures 6.2, 6.3, and 6.4. The remaining Graphs are included in the Appendix.



(a) Temperature over Time - Node B



(b) Temperature over Time - Node EXIT

Figure 6.1: Comparison of Nodal Temperatures over Time

6.1 Nodal Temperature over Time

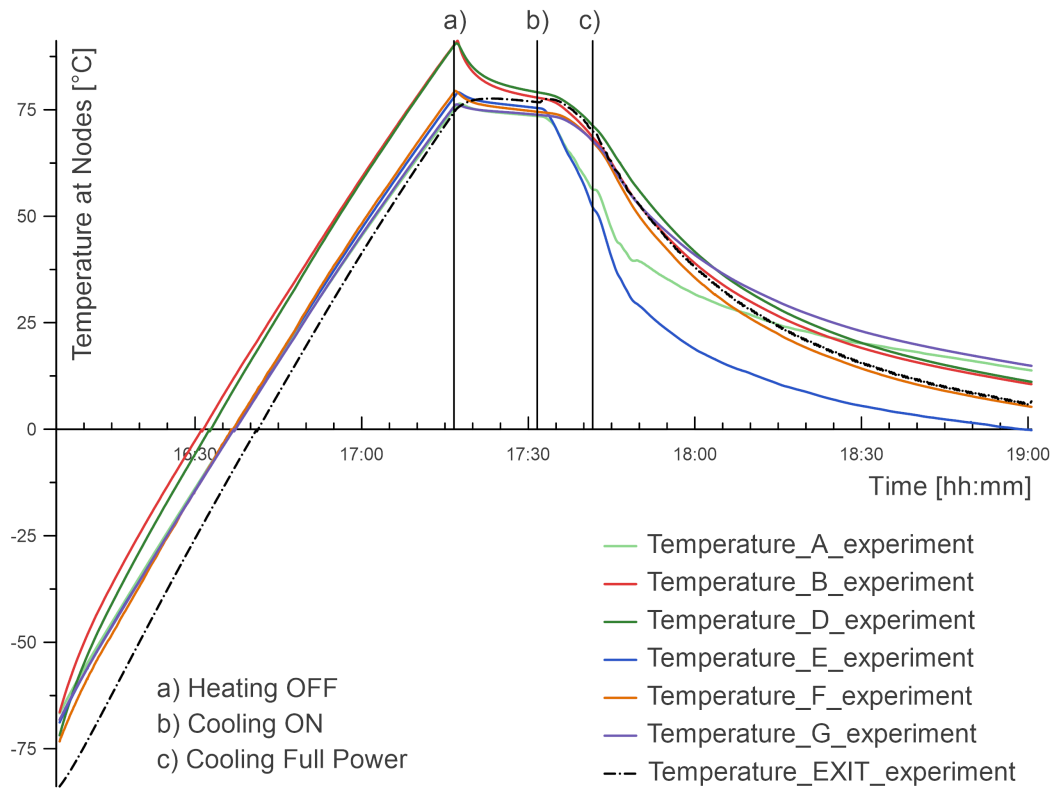


Figure 6.2: Temperature over Time - Experiment

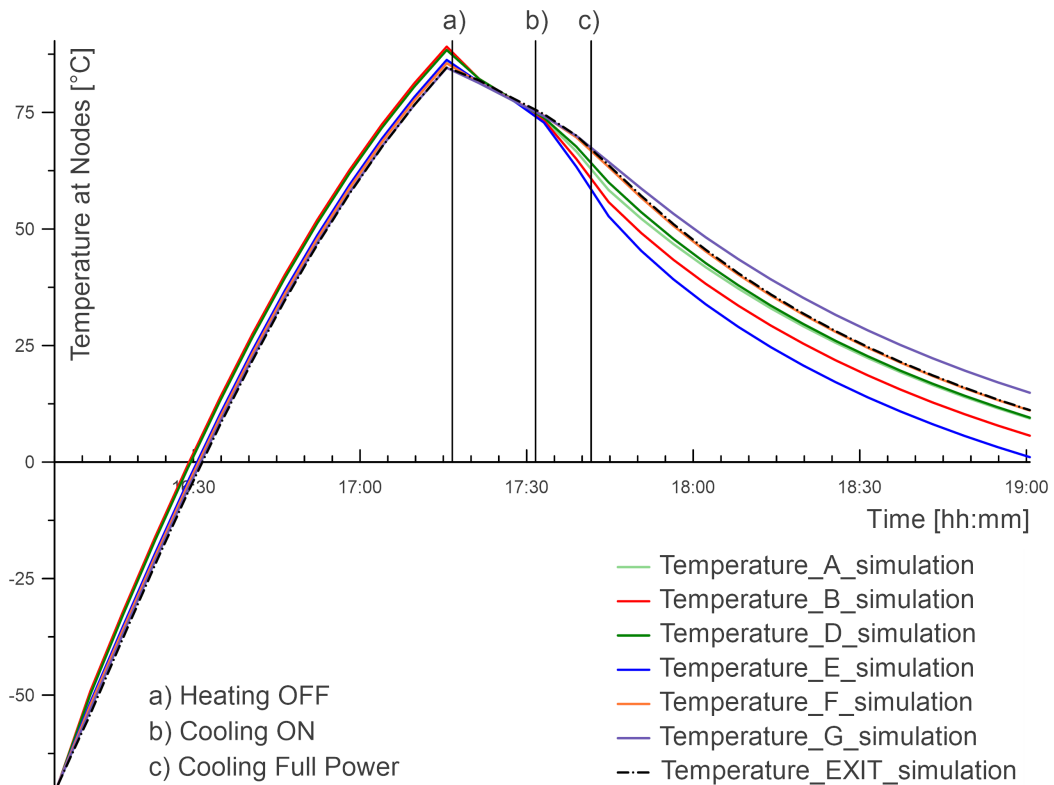


Figure 6.3: Temperature over Time - Simulation

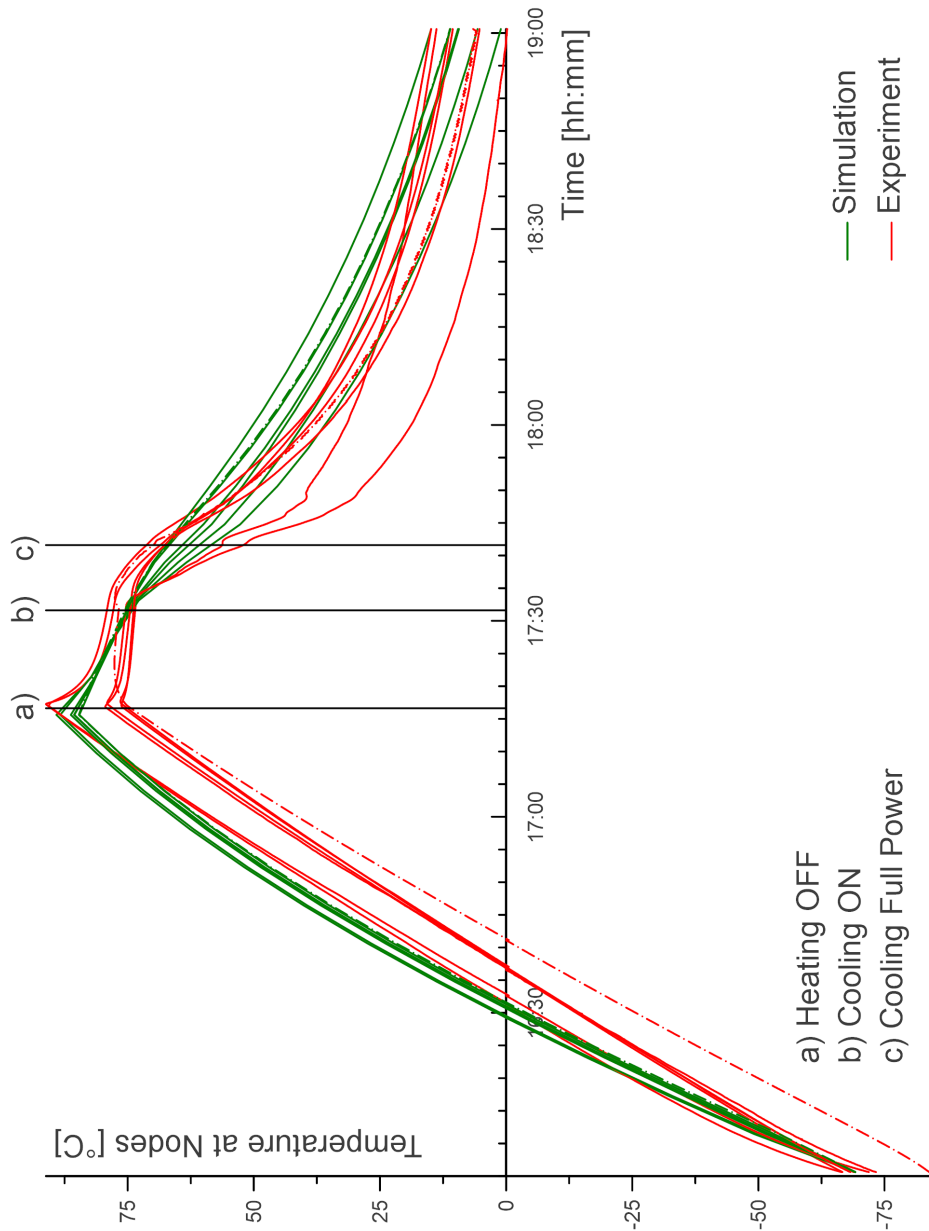


Figure 6.4: Combined Comparison of Nodal Temperatures over Time

6.2 Deviation from Experiment

To better visualise the changing disparity between simulation and experiment data, the whole data set was converted to Kelvin, and the deviation between each Nodal pair was calculated. This absolute difference between experiment and simulation for all Nodes is shown in Figure 6.5.

As relative differences may increase the understanding of this simulation's shortcomings, when compared to the ones realised in the future, they were computed and are shown in Figure 6.6.

Both maximal deviation and the arithmetic mean for each Node are listed in Table 10. minimal deviations are not included because for presented Nodes the minimal value is zero.

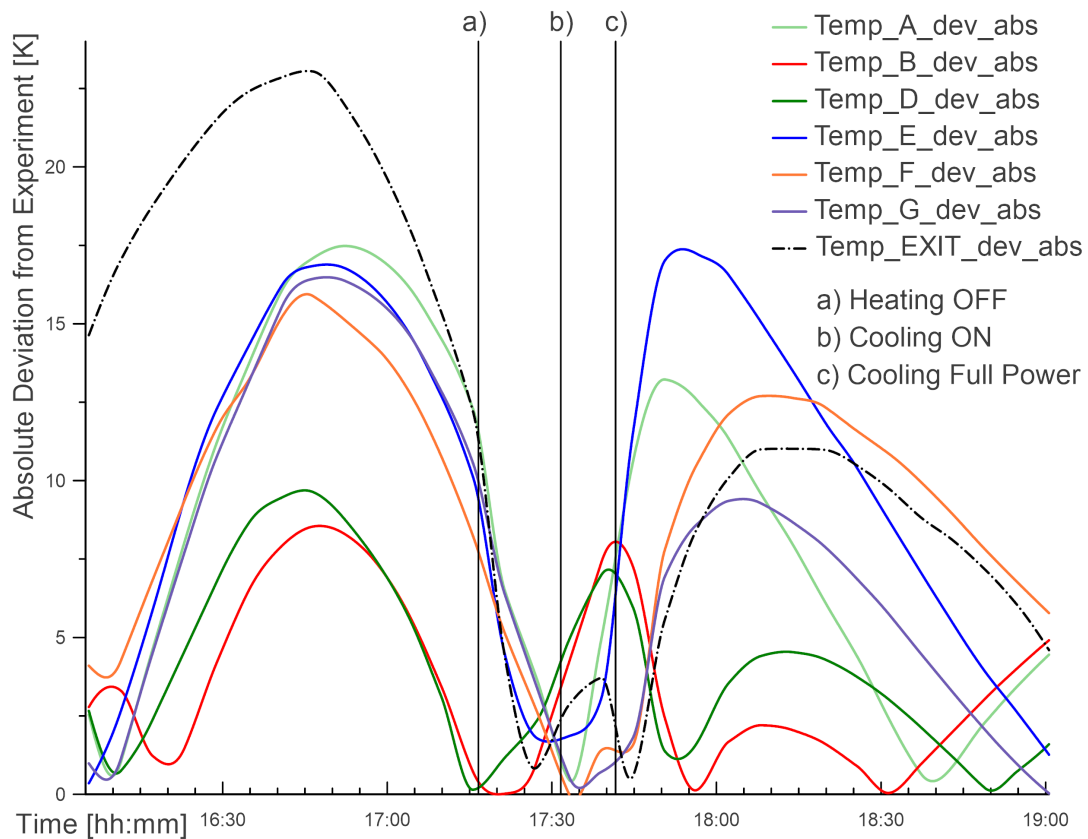


Figure 6.5: Deviation from Experiment [K]

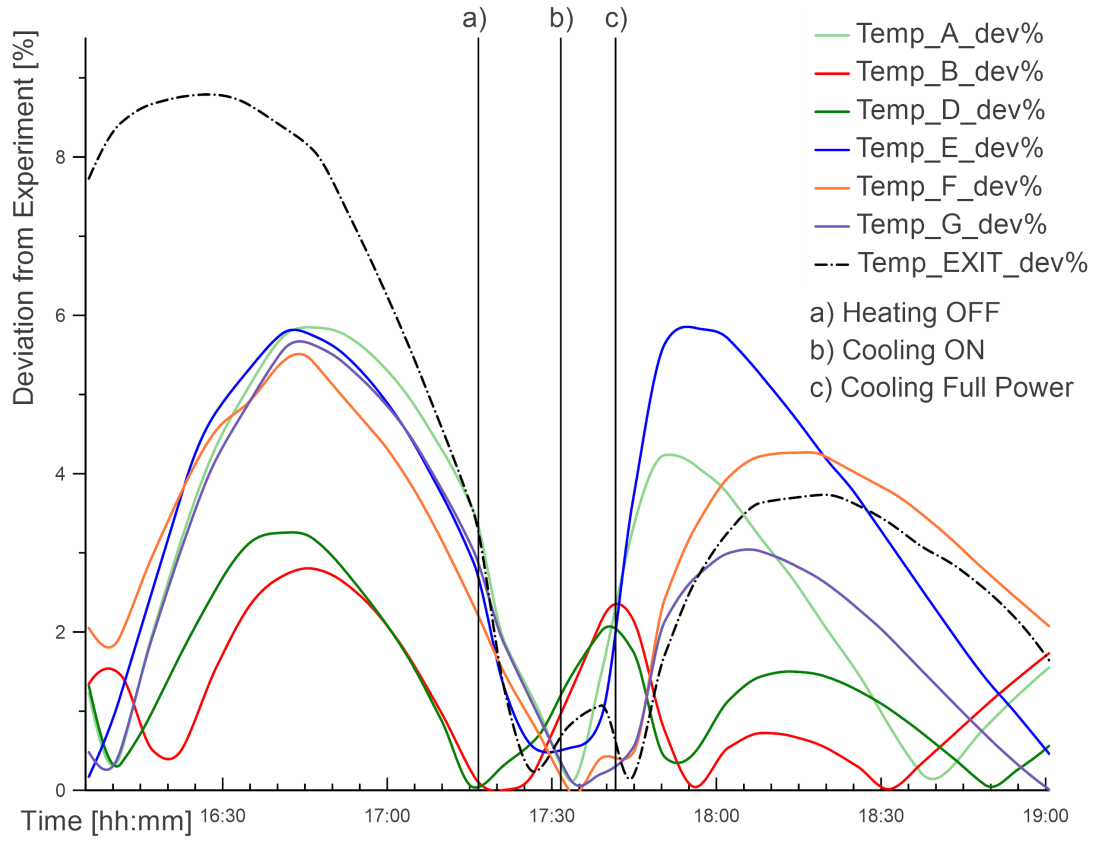


Figure 6.6: Deviation from Experiment [%]

Node	Deviation [K]	Mean [K]	Deviation [%]	Mean [%]
A	17.48	8.30	5.85	2.78
B	8.54	3.46	2.80	1.15
D	9.64	3.99	3.25	1.33
E	17.23	9.73	5.84	3.34
F	15.88	9.11	5.42	3.14
G	16.43	7.34	5.63	2.46
EXIT	23.04	12.03	8.79	4.41

Table 10: Nodal Deviation

6.3 Interpretation of Results

6.3.1 Heating Phase

Considering the thermal load the top plate is directly exposed to during the heating cycle, the curve expected should be concave, nearing linear. The results reflect that, however, simulation data shows a slightly greater gradient than experimental ones. This is most likely caused by a slight discrepancy in simulated thermal resistances between the two plates and between the main body and the bottom plate.

6.3.2 Dwell Phase

The dwell time between heating and cooling shows similar temperature loss for both the experiment and simulation, although the simulation data shows a much more linear development. Because no heat is introduced into the system in this stage, the variables influencing temperature change are the convection coefficient, the thermal resistance, and the radiation emissivity. Fine-tuning of these parameters would be necessary for a more accurate result.

6.3.3 Cooling Phase

Comparing the shape of the cooling curves (fig. 6.4) there is a noticeable difference which would suggest a diverging trend in a longer cooling cycle. That is a worrying discovery that would suggest a non-negligible problem in the boundary conditions. One possible source of deviation could be a non-zero flow of liquid nitrogen into the system. One of the assumptions made was that all nitrogen entering the chamber is already in a gaseous state. The dual state flow this would introduce would change the cooling mechanism and with the increasing ratio of liquid nitrogen diverge the experimental results from the simulation. To account for this issue next experiment should include an expansion chamber.

Another variable that affects the shape of the cooling curve is the convection coefficient between the gaseous nitrogen and aluminium body. To obtain this value more precisely it would have to be experimentally determined which is outside of the scope of this thesis.

7 Conclusion

This thesis aimed to create a Thermal-Flow Simulation design that accurately mimicked a real-life experiment in hopes to reduce experimental costs and setup time. It included a model assembly, mesh generation, solution parameters, and the incorporation of boundary conditions.

The beginning of the thesis contains research summarising the field of Thermal-Vacuum testing. It includes the types of tests and their requirements, the used test equipment, and the means of simulating thermal, pressure, and solar environments.

The following research covers the fundamentals of mathematical modelling, finite element analysis, computational fluid dynamics, and the equations governing thermal flow.

The practical section of the thesis attends to the development of the simulation and its validation experiment.

Experiment and simulation data analysis showed maximal nodal temperature differences between 8.54 and 23.04 Kelvin, which is already usable for future pre-experiment simulations. This is supported by the fact, that any subject tested, will most likely be placed in the middle of the plate, which corresponds to the nodes with the lowest deviations (B and D).

In summary, the presented simulation is capable of accurately predicting the temperature profile of a cold plate inside of a Thermal-Vacuum Chamber and can be used for future experiments that include test subjects inside the chamber.

This work can be built upon by experimentally determining the emissivity and absorptivity of used aluminium and the convection coefficient inside the labyrinth, fine-tuning the thermal resistance between aluminium parts, and adding an expansion chamber to the real-life experimental setup.

List of symbols

Symbols

A	area
$\frac{D}{Dt}$	material derivative
e	emissivity
\mathbf{g}	body accelerations
h_c	heat transfer coefficient
k	thermal conductivity
\bar{p}	modified pressure
Q	quantity of heat
t	time
T	temperature
\mathbf{u}	flow velocity
x	component in the x direction
y	component in the y direction
z	component in the z direction
δ	Stefan-Boltzmann constant
μ	dynamic viscosity
ρ	fluid density
σ_{ij}	Cauchy stress tensor

Abbreviations

CTU	Czech Technical University
NASA	National Aeronautics and Space Administration
ESA	European Space Agency
LN_2	Liquid Nitrogen
GN_2	Gaseous Nitrogen
LASP	Laboratory for Atmospheric and Space Physics
CAD	Computer Aided Design
FEA	Finite Element Analysis
CFD	Computer Fluid Dynamics

List of Figures

2.1	Space Environment in proximity to Earth [5]	2
2.2	Examples of Simulation Chambers	7
2.3	Examples of Vacuum Pumps	9
2.4	Solar Environment Simulation Technology	11
2.5	Bayard-Alpert Ion Gauges [18]	11
3.1	CTU Thermal-Vacuum Chamber	15
4.1	Thermal Control System Experiment Setup	18
4.2	Temperature over Time - Full Experimental Data Set	19
5.1	Model Assembly	21
5.2	Examples of meshed parts	22
5.3	Solution Parameters	23
5.4	Examples of used Boundary Conditions	26
5.5	Simulation Results	28
6.1	Comparison of Nodal Temperatures over Time	29
6.2	Temperature over Time - Experiment	30
6.3	Temperature over Time - Simulation	30
6.4	Combined Comparison of Nodal Temperatures over Time	31
6.5	Deviation from Experiment [K]	32
6.6	Deviation from Experiment [%]	33

List of Tables

1	Space Environment in proximity to Earth [4]	2
2	Comparison between rules and standards [6]	5
3	List of Thermal Conditioning Options [13]	6
4	Working ranges of vacuum pumps [21]	10
5	Working ranges of vacuum gauges [25]	12
6	Experiment Cycle Details	19
7	Main Dimensions	20
8	Mesh Parameters	22
9	Boundary Conditions	25
10	Nodal Deviation	33

Appendix

Attachment 1: Simulation Archive

Attachment 2: Drawing of Sensor Positions

Attachment 3: Graph of Temperature over Time - Node B

Attachment 4: Graph of Temperature over Time - Node D

Attachment 5: Graph of Temperature over Time - Node E

Attachment 6: Graph of Temperature over Time - Node F

Attachment 7: Graph of Temperature over Time - Node G

Attachment 8: Contour Plot showing Fluid Velocity inside the Labyrinth

Attachment 9: Contour Plot showing Maximal Reached Temperature

References

- [1] W. Hallmann W. Ley K. Wittmann. *Handbook of Space Technology*. 2009. ISBN: 978-0-470-69739-9.
- [2] NASA. *NASA Spacecraft Classification [online]*. accessed Oct 24 2020. URL: https://www.nasa.gov/audience/forstudents/postsecondary/features/F_Spacecraft_Classification.html.
- [3] Department of Defense. *Product Verification Requirements for Launch, Upper-Stage, and Space Vehicles*. Jan 15 1999.
- [4] C. de O. Lino R. S. S. Chisabas G. Loureiro. "Space Thermal and Vacuum Environment Simulation [online]". In: *Space Flight*. IntechOpen, 2018. URL: <https://doi.org/10.5772/intechopen.73154>.
- [5] Vincent L. Pisacane. *Fundamentals of Space Systems*. 2005. ISBN: 978-0-19-516205-9.
- [6] R.S.S. Chisabas et al. "Method for CubeSat Thermal-Vacuum Cycling Test Specification". In: (Jul 20 2017).
- [7] European Cooperation for Space Standardization. *Space Engineering: Verification*. Mar 2009.
- [8] NASA Goddard Space Flight Center. *General Environmental Verification Standard*. Apr 22 2013.
- [9] Department of Defense. *Test Requirements for Launch, Upper-Stage, and Space Vehicles Vol.I: Baselines*. Jul 01 1985.
- [10] European Cooperation for Space Standardization. *Space Engineering - Testing*. Jun 1 2012.
- [11] Air Force Space Command. *Test Requirements for Launch, Upper-Stage, and Space Vehicles*. Sep 5 2014.
- [12] R.S.S. Chisabas et al. "Development of a Thermal-Vacuum Chamber for testing in Small Satellites". In: (Jul 20 2017).
- [13] Bemco Inc. *Environmental Chambers and Space Simulation Systems*. accessed Nov 16, 2020. URL: <http://www.bemcoinc.com/AH.htm>.
- [14] Laboratory for Atmospheric and Space Physics. *Vacuum Test Chambers [online]*. accessed Nov 12, 2020. URL: https://lasp.colorado.edu/home/engineering/facilities/vacuum/?doing_wp_cron=1478624411.6843330860137939453125.
- [15] TriasRnD. *Space Simulation Chamber (TVAC) [online]*. accessed Nov 12, 2020. URL: <https://triasrnd.com/en/1/63-space-simulation-chamber-tvac>.
- [16] R. S. S Chisabas. *Space simulation chambers state-of-the-art*. 30 Sep 2016.

REFERENCES

- [17] L. Brieda et al. *Outgassing Characterization of Rod Heaters used for GOES-R Thermal Vacuum Testing [online]*. accessed Oct 23, 2020. URL: <https://core.ac.uk/download/pdf/162000482.pdf>.
- [18] Ideal Vacuum Products. *Vacuum Technology [online]*. accessed Nov 12, 2020. URL: <https://www.idealvac.com>.
- [19] Compressor World. *Powerex 5HP Scroll Pump [online]*. accessed Nov 12, 2020. URL: <https://www.compressorworld.com>.
- [20] Czech Museum of Mass Spectrometry. *Vacuum Technology [online]*. accessed Nov 12, 2020. URL: <https://www.ms-museum.org/diffusion-pump-edwards>.
- [21] W. Umrath. *Fundamentals of Vacuum Technology*. 1998. ISBN: 978-5881359867.
- [22] NATO AGARD. *Space Simulation Chambers and Techniques*. 1964. DOI: 10.14339.
- [23] Atlant. *Xenon Short-Arc Lamp [online]*. accessed Nov 12, 2020. URL: https://commons.wikimedia.org/wiki/File:Xenon_IMAX_1.jpg.
- [24] mks Newport. *Simulation of Solar Irradiation [online]*. accessed Nov 12, 2020. URL: <https://www.newport.com/n/simulation-of-solar-irradiation>.
- [25] B. S. Halliday A. Chambers R. K. Fitch. *Basic Vacuum Technology*. 1998. ISBN: 0 7503 0495 2.
- [26] European Cooperation for Space Standardization. *Space Product Assurance - Detection of organic contamination of surfaces by infrared spectroscopy*. 2009.
- [27] Mark Bowen Thomas Witelski. *Methods of Mathematical Modelling*. Springer, Cham. ISBN: 978-3-319-23042-9.
- [28] Clive A.J. Fletcher. *Computational Techniques for Fluid Dynamics 2: The Governing Equations*. 1991. ISBN: ISBN 978-3-642-58239-4.
- [29] Jiří Šimůnek. *Numerický model dvourozměrného proudění kapaliny a rozpuštěných látek v nenasyceném pórovitém prostředí*. 1993.